Vol 13 No 9, September 2004
1009-1963/2004/13(09)/1428-04

Chinese Physics

© 2004 Chin. Phys. Soc.
and IOP Publishing Ltd

# Holographic grating formation in dry photopolymer film with shrinkage*

Luo Shou-Jun(骆守俊)[a)†], Liu Guo-Dong(刘国栋)[a)], He Qing-Sheng(何庆声)[a)], Wu Min-Xian(邬敏贤)[a)], Jin Guo-Fan(金国藩)[a)], Shi Meng-Quan(施盟泉)[b)], Wang Tao(王 涛)[b)], and Wu Fei-Peng(吴飞鹏)[b)]

[a)] *State Key Laboratory of Precision Measurement Technology and Instruments, Tsinghua University, Beijing* 100084, *China*

[b)] *Technical Institute of Physics and Chemistry, Chinese Academy of Sciences, Beijing* 100101, *China*

(Received 22 December 2003; revised manuscript received 28 April 2004)

An important issue in developing applications for photopolymers in holography is the effect of shrinkage on recording properties. In this paper, we introduce a model to describe real-time formation of a single grating in photopolymers at any geometrical angle, under the assumption that the shrinkage is in proportion to the polymerization. This model combines polymerization kinetics with the coupled-wave theory, explaining the shrinkage effect on the diffraction efficiency. The model is validated by comparing its predictions with the experimental results for a film of 99$\mu$m thickness.

**Keywords:** photopolymer, holographic grating, shrinkage
**PACC:** 4240E

## 1. Introduction

Photopolymerizable materials are of considerable interest for development of holographic data storage devices because of their high sensitivity, high resolution, long shelf life, dry real-time processing, and low cost.[1−3] A number of photopolymerizable materials for holographic applications have been developed.[4−6] One problem with photopolymers is that the materials shrink during polymerization, leading to Bragg mismatch at read-out. Some methods have been suggested to reduce the effect of shrinkage.[7,8] However, it is not possible to eliminate the effect of shrinkage in all materials for polymerization.

Several models have been presented in the literature to describe the effect of material shrinkage. They include (1) the fringe-plane rotation model,[9] (2) the average refractive-index change model,[10] and (3) the fringe-plane rotation and average refractive-index change model.[11] In all these models it is assumed that at least one side of the material is attached to a rigid glass substrate. Also it is assumed that shrinkage occurs only along the direction normal to the material's surface.

This paper describes a dynamic model of single-grating formation in photopolymers at any geometrical angle, based on the fringe-plane rotation model. Different from those conventional models, this model will aid the understanding and optimization of the recording of complex hologram in shrinkable photopolymer. The control of the hologram recording process is a critical issue for these materials.

## 2. Theory

In our model, we only discuss the effect of shrinkage along the direction of the normal to the material's surface because the shrinkage in the lateral (in-plane) directions is much smaller owing to anchoring of the photopolymer to the glass substrate during exposure.[12,13]

As shown in Fig.1, two coherent plane waves (polarized normal to the plane of incidence) with constant intensities $I_1$ and $I_2$ along the vector $\boldsymbol{k}_d$ and $\boldsymbol{k}_p$ interfere with each other in a holographic recording material. $\theta_{\rm s}$ and $\theta_{\rm f}$ are their incident angles inside the film. With the photopolymerization initiating, the thickness $d$ has a shrinkage $\alpha(t)$ and the holographic

*Project supported by the State Key Development Programme for Based Research of China (Grant No G1999033001), and the National Natural Science Foundation of China (Grant No 60277011).

†Corresponding author: luosj02@mails.tsinghua.edu.cn

gratings $\boldsymbol{K}_{\mathrm{g}}$ recorded in different time are also changing. For very small shrinkage (~2–3%),[14] we only consider that the gratings recorded before are transformed into the same $\boldsymbol{K}'_{\mathrm{g}}(t)$. Correspondingly, the grating period $\Lambda_0 = \Lambda(0)$ and the grating slant angle $\theta_0 = \theta(0)$ are transformed into $\Lambda(t)$ and $\theta(t)$ respectively.

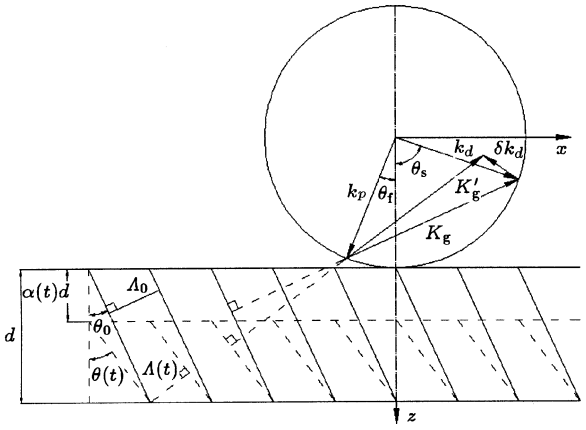



**Fig.1.** The Bragg deviation introduced by the shrinkage along the direction of the normal to the photopolymer's surface.

When the photopolymerization is initiated, the rate of free monomer consumption is described by [15]

$$\frac{\mathrm{d}}{\mathrm{d}t}u(t) = -k_{\mathrm{R}}(t)u(t)(I_1 + I_2)^{\delta}, \tag{1}$$

where $u(t)$ is the free-monomer spatial average density, $\delta$ is the order of the photochemical reaction, $k_{\mathrm{R}}(t)$ is the characteristic rate coefficient, which depends on the ratio of the free-monomer polymerization rate to the polymeric-chain termination rate.[15] From Ref.[16], we obtain $k_{\mathrm{R}}(t) = k_0 \exp(t/\tau)$, where $k_0 \equiv k_{\mathrm{R}}(0)$ and $\tau$ is the time constant.

Solving Eq.(1), given $u(0) = u_0$, $u(\infty) = 0$ and $p(t) = u_0 - u(t)$ as the spatial average photopolymer density, we obtain

$$p(t) = u_0 \left\{1 - \exp\left[\gamma(1 - \exp(t/\tau))\right]\right\}, \tag{2}$$

where $\gamma = (I_1 + I_2)^{\delta} k_0 \tau$ is a positive constant responsible for the time evolution. Under the assumption that the shrinkage is in proportion to the polymerization, we obtain the shrinkage rate $\alpha(t)$:

$$\alpha(t) = \alpha_{\mathrm{M}} \left\{1 - \exp\left[\gamma(1 - \exp(t/\tau))\right]\right\}, \tag{3}$$

where $\alpha_{\mathrm{M}}$ is the available maximum of $\alpha(t)$. Then the deviation of Bragg angle is given by[17]

$$\begin{aligned}
&\Delta\theta(t) \\
&= \theta(t) - \theta_0 = \tan^{-1}\left(\frac{\tan\theta_0}{1 - \alpha(t)}\right) - \theta_0 \\
&= \tan^{-1}\left(\frac{\tan\theta_0}{1 - \alpha_{\mathrm{M}}\left\{1 - \exp\left[\gamma(1 - \exp(t/\tau))\right]\right\}}\right) - \theta_0.
\end{aligned} \tag{4}$$

The results deduced from Eq.(4) are used to predict the deviation of Bragg angle during the process of exposure, and some compensation can be obtained by adjusting the angle of readout beam.

The modulation index $\Delta n(t)$ is described by[16]

$$\Delta n(t) = \Delta n_{\mathrm{M}} m \left(1 - \exp\left\{\gamma[1 - \exp(t/\tau)]\right\}\right), \tag{5}$$

where $\Delta n_{\mathrm{M}}$ is the maximum available of modulation index and $m = 2\sqrt{I_1 I_2}/(I_1 + I_2)$ is the modulation intensity.

From Ref.[18], we obtain

$$\eta = \sin^2\left(\frac{\pi d n_0 \Delta n(t)}{\lambda\sqrt{\cos\theta_{\mathrm{s}}\cos\theta_{\mathrm{f}}}}\right) \mathrm{sinc}^2\left(\frac{d\delta\boldsymbol{k}_d \cdot \hat{z}}{2\pi}\right), \tag{6}$$

where $n_0$ is the average refractive index of the material and $\lambda$ is the free-space wavelength, $\hat{z}$ is the unit vector of $z$-axis. $\delta\boldsymbol{k}_d = \boldsymbol{k}_p - \boldsymbol{k}_d + \boldsymbol{K}'_{\mathrm{g}}(t)$ is the Bragg mismatch vector.

According to the geometry relation, the shrinkage can be described as

$$\alpha(t) = \frac{\sin(\theta(t) - \theta_0)}{\sin\theta(t)\cos\theta_0}, \tag{7}$$

$$\Lambda(t) = \Lambda_0 \frac{\cos\theta(t)}{\cos\theta_0}, \tag{8}$$

$$\delta\boldsymbol{k}_d = \boldsymbol{k}_p - \boldsymbol{k}_d + \boldsymbol{K}'_{\mathrm{g}}(t) = \boldsymbol{K}'_{\mathrm{g}}(t) - \boldsymbol{K}_{\mathrm{g}}. \tag{9}$$

The value of grating vector is

$$K'_{\mathrm{g}}(t) = 2\pi/\Lambda(t). \tag{10}$$

From Eqs.(7)–(10), we obtain:

$$\begin{aligned}
\delta\boldsymbol{k}_d \cdot \hat{z} &= \frac{2\pi}{\Lambda(t)}\sin\theta(t) - \frac{2\pi}{\Lambda_0}\sin\theta_0 \\
&= \frac{\alpha(t)}{1 - \alpha(t)}\frac{2\pi}{\Lambda_0}\sin\theta_0.
\end{aligned} \tag{11}$$

Finally, we can obtain the real-time evolution of diffraction efficiency:

$$\eta(t) = \sin^2\left(\frac{\pi d n_0 \Delta n(t)}{\lambda\sqrt{\cos\theta_s \cos\theta_f}}\right) \times \mathrm{sinc}^2\left(\frac{\alpha(t) d \sin\theta_0}{[1-\alpha(t)]\,\Lambda_0}\right)$$

$$= \sin^2\left(\frac{\pi d n_0 \Delta n_M m\,(1-\exp\{\gamma[1-\exp(t/\tau)]\})}{\lambda\sqrt{\cos\theta_s \cos\theta_f}}\right) \times \mathrm{sinc}^2\left(\frac{\alpha_M\{1-\exp[\gamma(1-\exp(t/\tau))]\}\, d \sin\theta_0}{(1-\alpha_M\{1-\exp[\gamma(1-\exp(t/\tau))]\})\,\Lambda_0}\right). \quad (12)$$

# 3. Experiment

## 3.1. Preparation of photopolymer

In this experiment, a film with a thickness of 99$\mu$m was prepared as follows: the monomers: 2-benzoxyethyl acrylate (POEA) (29.2%wt) and N-vinyl cabazole (NVC) (17.2%); chain transfer agent: 4-methyl-4H-1, 2, 4-triazole-3thiol (MMT) (1.92%wt); photosensitizer dye 2, 5-bis[[4-(dimethylamino)-phenyl] methylene]-cyclopentanone (DMAW) (0.07%wt); initiator 1, 1', 2, 2'-bis (o-chlorophenyl)-4, 4', 5, 5'-tetraphenyl-bisimidazole (o-cl-HABI) (1.2%wt); polymeric binder: poly(vinyl acetate) (50.4%). Dichloromethane is used as solvent. The solution was coated onto a glass plate with a thickness of 0.8mm by using a spin coater. Different rotation speeds were used to obtain various coating thickness. Coated samples were dried in vacuum for 24h at 20–24°. The average refractive index $n_0$ of the films with a thickness of 99$\mu$m is about 1.5, and its maximum of shrinkage $\alpha_M$=2.6%.

## 3.2. Experimental results and discussion

As shown in Fig.2, the film is mounted on a rotation stage. The optical system for recording the grating structure provides two collimated beams derived from an argon-ion laser at 514.5nm. The angle between object beam and reference beam outside the material is 22°C. The intensities of reference and object beams are both adjusted to 11.2mW/cm$^2$. We sample the diffractive intensity at the frequency of 0.1Hz by turning on and off the shutters. Four different rotation angles have been chosen, and at each rotation angle $\varphi$, about 30 samplings are collected by the detector, equipped with a computer.

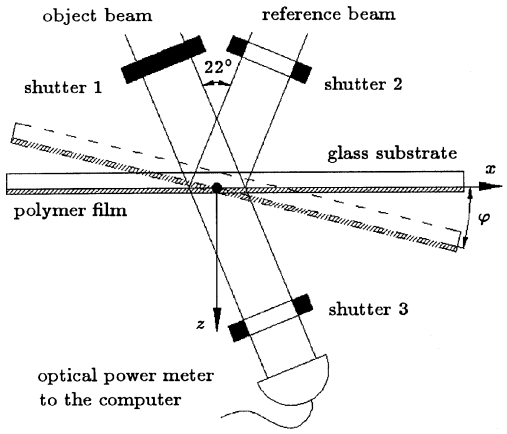



**Fig.2.** Schematic diagram of the setup used for examining the shrinkage effect on the diffraction efficiency at different rotation angle $\varphi$ of photopolymer film which is mounted on a rotation stage.

Different $\varphi$ corresponds different $\theta_s$, $\theta_f$, $\theta_0$

$$\theta_s = \sin^{-1}(\sin(11^\circ + \varphi)/n_0),$$
$$\theta_f = \sin^{-1}(\sin(11^\circ - \varphi)/n_0),$$
$$\theta_0 = (\theta_s - \theta_f)/2.$$

And $\Lambda_0$ can be calculated:[19]

$$\Lambda_0 = \lambda/(2\sin 11^\circ) = 1.35\mu\mathrm{m}.$$

When an unslanted grating is recorded, the fringe is formed normal to the surface of the recording material and the fringe-plane does not rotate during the process of photopolymer's shrinkage. The period of the grating will not change because the shrinkage in the lateral directions is much smaller than that in the direction normal to the material's surface.[13] Therefore, Eq.(12) can be simplified as

$$\eta(t) = \sin^2\left(\frac{\pi d n_0 \Delta n_M m\,(1-\exp\{\gamma[1-\exp(t/\tau)]\})}{\lambda\sqrt{\cos\theta_s \cos\theta_f}}\right). \quad (13)$$

In order to obtain the values of parameters $\gamma$, $\tau$, $\Delta n_M$, we fit the experimental curve with $\varphi = 0^\circ$ using the curve plotted according to Eq.(13). The obtained values of $\gamma$, $\tau$, $\Delta n_M$ are 1.54, 85.8s, and $1.1\times10^{-3}$ respectively. Next, the corresponding predictions (solid curves) according to Eq.(12) and the measured values

(dotted curves) are plotted in Fig.3 at different rotation angle $\varphi$. The good agreement between theory and experiment validates our dynamic model. The small deviation of the experimental curves from the theoretical ones is due to the optical quality of the photopolymer film's surface and the small fluctuation of laser power during the exposure.

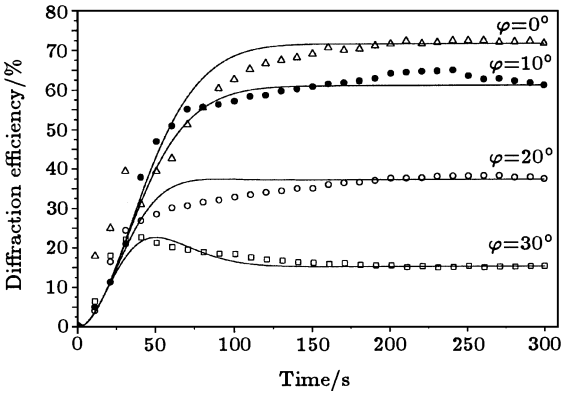



**Fig.3.** Comparison between theoretical curves and the corresponding experimental results for the different rotation angle. $\varphi$

During the formation of the slanted grating, the refractive index modulation and the deviation of Bragg angle resulting from the photopolymer's shrinkage continuously increase until the polymerization is finished. They both lead to the change of diffraction efficiency with exposure time, especially at the rotation angle $\varphi = 30°$, as shown in Fig.3.

The curves in Fig.4 obtained from Eq.(4) describe the change of the deviation of Bragg angle with exposure time at the different rotation angle $\varphi$ under irradiations with same intensities. We conclude that the incremental rotation angle $\varphi$ increases the deviation of Bragg angle under the same exposure which leads to the corresponding decrease of the diffraction efficiency shown in Fig.3.

According to Eq.(12), the period of the grating has an important effect on the diffraction efficiency, because smaller $\Lambda_0$ means higher selectivity of Bragg angle.[20] A small deviation of Bragg angle will sharply diminish the diffraction efficiency.

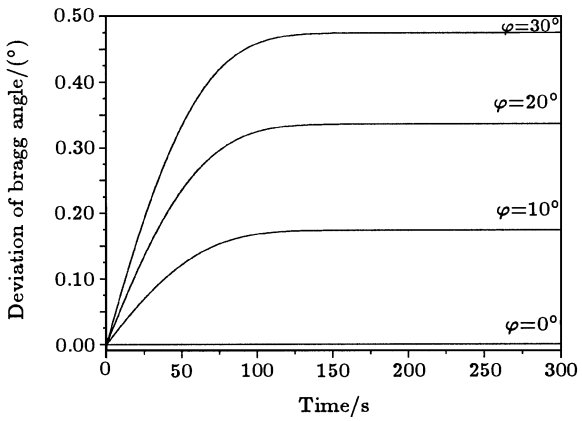



**Fig.4.** The deviation of Bragg angle versus the recording time under irradiation with an intensity of $I_1 = I_2$=11.2mW/cm$^2$.

# 4. Conclusion

Based on the fringe-plane rotation model, we combine the polymerization kinetics[15] with coupled wave theory[20] and introduce a dynamic model of single-grating formation in photopolymers at any geometrical angle, which is validated by comparing its predictions with the experimental results in a film of 99$\mu$m in thickness.

The obtained results are used to predict the effect of material shrinkage on the reconstruction of hologram recorded. Some compensation will be possible by adjusting the angle of reconstruction beam. The model also allows analysis of the influence of shrinkage rate on holographic recording diffraction efficiency.

Additionally, the model ensures that the diffraction efficiency after shrinkage can reach at least a local maximum by optimizing system parameters and adopting suitable exposure.

# References


[1] Smothers W K *et al* 1990 *Proc. SPIE* **1212** 20
[2] Rhee U S *et al* 1993 *Opt. Eng.* **32** 1839
[3] Yuan B H *et al* 2002 *Chin. Phys.* **11** 21
[4] Moreau V *et al* 2000 *Mater. Sci. Sem. Proc.* **3** 551
[5] Wilson W L *et al* 2000 *Opt. Quantum Electron.* **32** 393
[6] Hameed A Al Attar1 and Osama Taqatqa 2003 *J. Opt.* A: *Pure Appl. Opt.* **5** S487
[7] Steckman G J *et al* 1998 *Opt. Lett.* **23** 1310
[8] Waldman D A *et al* 1998 *Proc. SPIE* **3291** 89
[9] Vilkomerson D H R and Bostwick D 1967 *Appl. Opt.* **6** 1270
[10] Jordan M P and Solymar L 1978 *Electron. Lett.* **14** 271
[11] Fianla P *et al* 1987 *Proc. Soc. Photo-Opt. Instrum. Eng.* **747** 74
[12] Waldman D A *et al* 1997 *J. Imaging Sci. Technol.* **41** 497
[13] Shelby R M *et al* 2000 *Opt. Lett.* **25** 713
[14] Gallo J T and Verber C M 1994 *Appl. Opt.* **33** 6797
[15] Odian G 1970 *Principles of Polymerization* (New York: McGraw-Hill) p179
[16] Piazzolla S and Jenkins B 1996 *Opt. Lett.* **21** 1075
[17] Gallo J T and Verber C M 1994 *Appl. Opt.* **33** 6796
[18] Coufal H J 2000 *Holographic Data Storage* (New York: Springer) p36
[19] Goodman J W 1996 *Introduction to Fourier Optics* 2nd Edition (New York: McGraw-Jill) p321
[20] Kogelink H 1969 *Bell Syst. Tech. J.* **48** 2909